Structural colors from *Morpho peleides* butterfly wing scales

Yong Ding, Sheng Xu, and Zhong Lin Wang[a]

School of Materials Science and Engineering, Georgia Institute of Technology, Atlanta, Georgia 30332-0245, USA

A male *Morpho peleides* butterfly wing is decorated by two types of scales, cover and ground scales. We have studied the optical properties of each type of scales in conjunction with the structural information provided by cross-sectional transmission electron microscopy and computer simulation. The shining blue color is mainly from the Bragg reflection of the one-dimensional photonic structure, e.g., the shelf structure packed regularly in each ridges on cover scales. A thin-film-like interference effect from the base plate of the cover scale enhances such blue color and further gives extra reflection peaks in the infrared and ultraviolet regions. The analogy in the spectra acquired from the original wing and that from the cover scales suggests that the cover scales take a dominant role in its structural color. This study provides insight of using the biotemplates for fabricating smart photonic structures. © *2009 American Institute of Physics*. [doi:10.1063/1.3239513]

I. INTRODUCTION

Photonic crystals (PCs) are one of the most active research fields today.[1] They are a class of materials or structures in which the dielectric function or refraction index experiences a spatially periodic variation. The length scale of such variation, or their lattice parameter, determines the modulated spectral wavelength. For the photons with frequencies falling in the band gap of the PCs, the light can be totally reflected regardless its incidence direction, allowing it to propagate only along a specific direction, or even confining them within a specified volume. Utilizing optical and electron lithography, some complex photonic structures have been fabricated with one-, two-, and even three-dimensional structures.[2] However, due to the limitation of the hierarchical structures that can be created via lithography, the manmade PCs and their working wavelength ranges are rather limited.

In nature, tremendous numbers of living creatures, for example, some butterflies, beetles, and peacock, exhibit striking brilliancy colors.[3] Most of their colors, also named as structural colors, do not come from the pigments, but from their periodic nature-made PCs, or biophotonic materials. Such biologically self-assembled PCs are ideal examples, which can inspire us in design and fabrication of new photonic structures, and also can serve directly as biotemplates to mimic those structures.[4] *Morpho* butterfly wings are one of the most studied biophotonic materials. Although its iridescent feature has been investigated for more than a century, a major progress in physical interpretation has been achieved just after 1990s partially due to the development of measurement and characterization techniques and their technological applications.[5–19] For example, the applications of such nanostructures in *Morpho* butterfly wings have been successfully demonstrated for solar cells and gas sensors.[20,21]

Structurally, there are two types of scales on *Morpho* butterfly wings, which are named individually as cover and ground scales. The main structure on both scales is the ridges (or vanes) with periodically arranged shelves in each ridge. It is considered that the light reflection and interference from the shelves give their shining blue color.[3,13] The regularity and irregularity in the structures were further emphasized by Kinoshita and Yoshioka.[22] However, the different functions of cover and ground scales are still under debate. In this paper, using the male *Morpho peleides* butterfly as an example, the structural differences between the cover and ground scales have been explored by cross-sectional electron microscopy. The observed structures can be directly linked to the different reflection spectra acquired from the cover and ground scales. This study provides insight of using biotemplates for fabricating smart photonic structures.

II. EXPERIMENTS

The *Morpho peleides* butterflies were provided by the Day Butterfly Center in the Callaway Gardens, Georgia. Under optical microscope, the cover and ground scales were carefully separated, transferred, and periodically arranged on carbon tapes. The reflection spectra were acquired using a DU 640 spectrophotometer equipped with a reflection stage. The working wavelength range of the spectrophotometer covers from ultraviolet to infrared (200–1100 nm). A LEO 1550 scanning electron microscope (SEM) was used to characterize the surface morphology of the butterfly wings. For structure analysis, the butterfly wing was fully and entirely coated with alumina using atomic layer deposition (ALD) for enhancing the imaging contrast. After embedding the wings in epoxy, an ultramicrotome was used to slice the cross-sectional samples for analysis using transmission electron microscopy (TEM). The MIT photonic-band (MPB) package was used to calculate the band structure of the photonic structures.[23]

---

[a]Author to whom correspondence should be addressed. Electronic mail: zhong.wang@mse.gatech.edu.
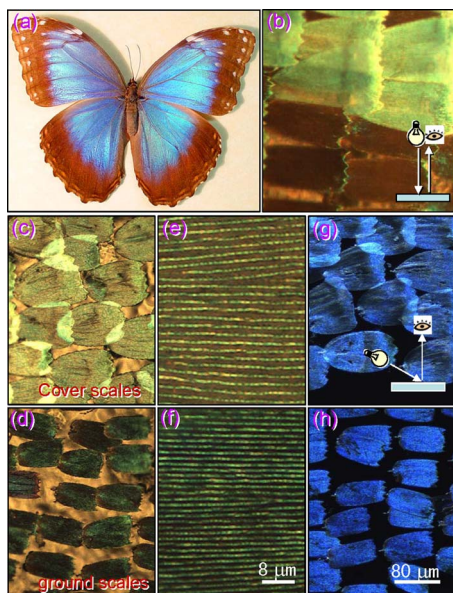
106, 074702-1

FIG. 1. (Color online) (a) An optical photograph of a male *Morpho peleides* butterfly. (b) An optical microscopy image of the scales on the wing at normal incidence. [(c) and (e) and (d) and (f)] Low and high magnification optical images of the cover and ground scales, respectively, when illuminated in the normal direction. [(g) and (h)] Optical images of the cover and ground scales, respectively, when illuminated from the side, as schematically shown in (g). The scales change colors with the change in illuminating direction.

III. RESULTS AND DISCUSSION

The colors from both cover and ground scales are orientation dependent. Figure 1 gives optical images of a male *Morpho peleides* butterfly wing in different scales and different incidence beam directions. With the white light illuminating from the top, the cover and ground scales on the wing display the yellow-green and brown colors, respectively [Fig. 1(b)]. After transferring them onto carbon tapes, the ground scales give dark green color in Fig. 1(d), while there is no big difference in cover scales [Fig. 1(c)]. The ridges can be seen clearly in the enlarged images of both cover and ground scales, as displayed in Figs. 1(e) and 1(f). When the white light illuminates from the side, both cover and ground scales give the shining blue color, as shown in Figs. 1(g) and 1(h), respectively.

Figure 2 gives SEM images of both cover and ground scales. The ridge separation distances in cover and ground scales are ~1.8 and ~1.7 μm, respectively. The periodically arranged shelves in each ridge can be seen more clearly in the cross-sectional views in Figs. 2(b) and 2(c), respectively. The trabeculae connect the shelves and the base plate together. Figures 2(d) and 2(e) present the enlarged top-view images of cover and ground scales, respectively. Based on the SEM images displayed in Fig. 2, the major structural difference between the cover and ground scales is the density of the cross ribs in between two nearby ridges. The density of the cross ribs in ground scale is almost twice of those in the cover scale. Further, more and larger trabeculae are arranged to connect the cross ribs with its base plate in ground scales. Later, we will see that such structure will affect their reflection spectra tremendously.
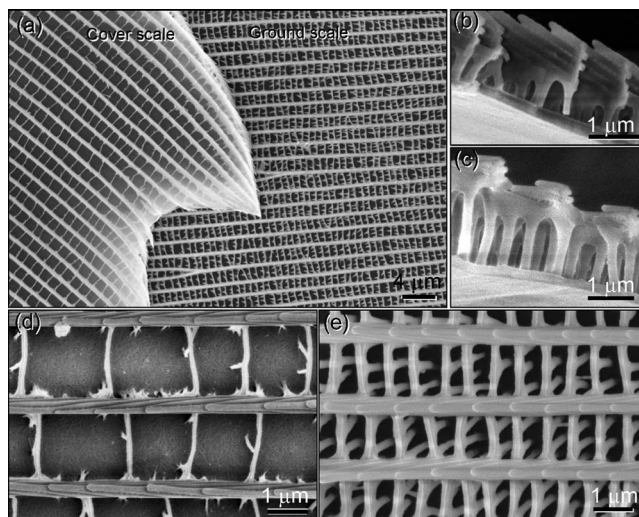

FIG. 2. (a) A low-magnification SEM image contains both the cover and ground scales. (b) and (c) are the cross-sectional SEM images; (d) and (e) are the plane-view SEM images of the cover and ground scales, respectively.

In order to explore the three-dimensional structure of the scales, the cross-sectional samples were prepared and investigated by TEM, which are displayed in Fig. 3. The cross-sectional images of the cover and ground scales viewing along their ridges (e.g., the slicing is perpendicular to the ridge, as shown in Fig. 2) are displayed in Figs. 3(a) and 3(b), respectively. Their flat base plates have a thickness around 250 nm. In each ridge, connected by a pillar, normally there are four shelves with thickness of its cuticle lamella and air layer, respectively, close to 90 and 70 nm. However, the ground scale has larger sized trabeculae and its base plate is heavily covered by the cross ribs. The cross-sectional images with viewing direction perpendicular to
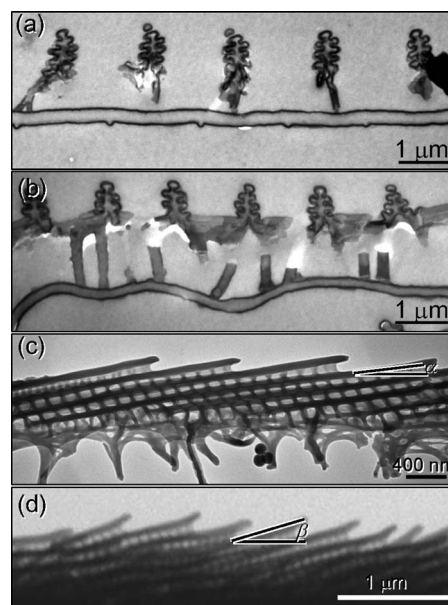

FIG. 3. Cross-sectional TEM images of the [(a) and (c)] cover and [(b) and (d)] ground scales viewing along and perpendicular to the ridges, respectively. The samples used for TEM imaging were coated with a thin layer of alumina by ALD. The inclination angles α and β of the shelf to scale surface in cover and ground scales are close to 7° and 17°, respectively.
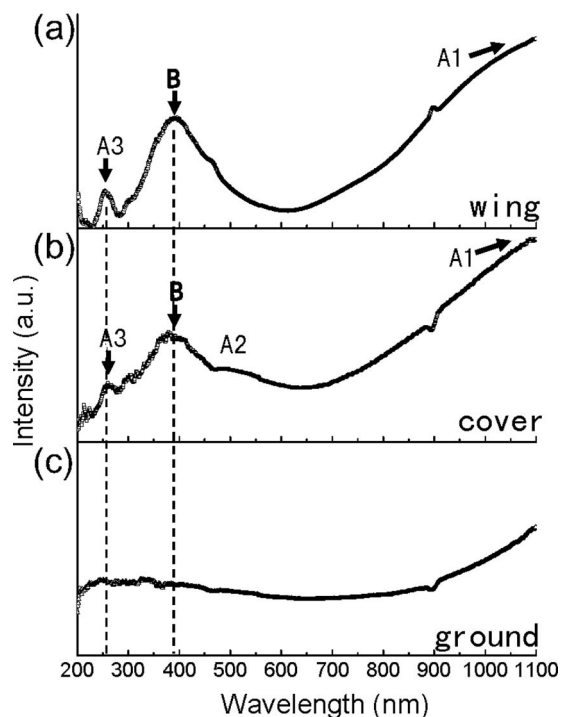
FIG. 4. Reflection spectra of the (a) original wing, (b) pure cover, and (c) pure ground scales with incidence angle as 33° from the tail direction. The tiny peaks and bumps at 466 and 896 nm are from the measurement system.
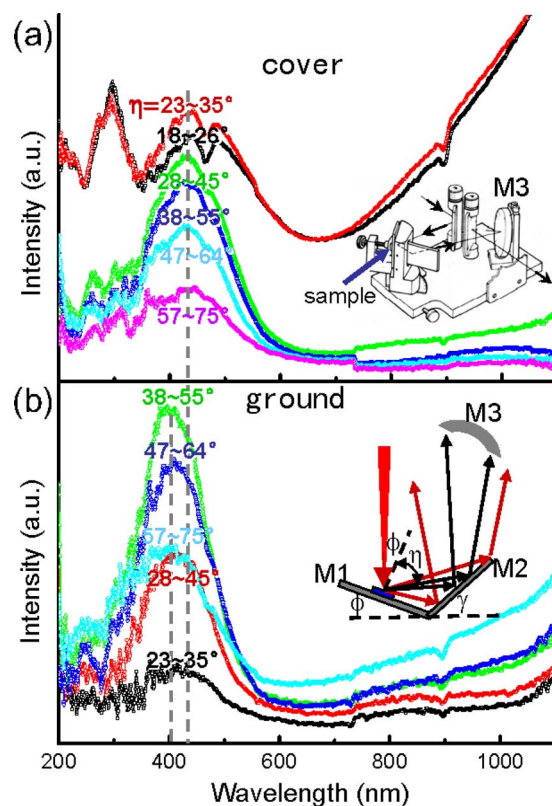

FIG. 5. (Color online) The reflection spectra measured from the (a) cover and (b) ground scales as a function of detector angle, with a fixed angle of 13° for the incidence beam from the tail direction. The inset in (a) is the experimental setup. The inset in (b) is an in-plane optical diagram for the measurements.

their ridges (e.g., the slicing is parallel to the ridge, as shown in Fig. 2) are shown in Figs. 3(c) and 3(d). A new structural feature is the subribs, which connect the shelves in each ridge. From this view direction, the inclination angles of each shelf relative to the surface or the base plate are measured to be 7° and 17° in the cover and ground scales, respectively. For description convenience, we define the direction from up to down side of the inclined shelf as tail to head (such direction is actually pointing to the head of the butterfly) since the reflection spectra acquired with incidence beams from the head and tail directions are different.

A set of reflection spectra in standard setting (relative to the normal direction of surface, the angles of the beam incidence and reflection detection are the same) from original wing, pure cover, and pure ground scales is displayed in Fig. 4. The incidence and reflection beams are kept in the same plane of the ridges with an incidence angle of 33° from the tail direction. The spectra from original wing and pure cover scales are analogous, while there was no well developed peak observed in the ground scale spectrum. There are three dominant peaks in Figs. 4(a) and 4(b), located around 259 nm (A3), 385 nm (B), and above 1100 nm (A1). The asymmetric shape of peak B indicates that it may be the summation of two separated peaks (A2 and B). With the incidence angle increasing, peaks A1, B, and A3 show blueshift and their corresponding wavelengths in original wing and pure cover scales are consistent. Still, there is no peak observed in the spectra of the ground scales even with the incidence angle changes.

It is obvious that the ground scales can give the blue color as the cover scales shown in Fig. 1. In order to understand why no peak is showing up in the reflection spectra of

the ground scales, in Fig. 5, by changing the detection azimuth, we measured the angular distribution of the reflection from both cover and ground scales while the incidence angle was fixed at 13° from the tail direction. The sketch of our reflection stage is inserted in Fig. 5(a), while its top-view optical diagram is inserted in Fig. 5(b). The sample is mounted at the M1 mirror position, the reflection departed from the sample will be further reflected by M2 mirror, and only the beams arriving at the M3 concave mirror (as indicated by dark arrow heads) will reach the detector and be counted in each spectrum. The angle ϕ is the incidence angle, which is 13° here. The convergence of the incidence beam is $\pm 4.6°$, which determines our detection error. Because we use a concave mirror to collect the reflected beam, the spectrum acquired at each setting of ϕ and γ corresponds to an angular distribution of the reflection. With a fixed angle ϕ, the ranges of the detected reflection will shift with the change in angle γ. With a fixed incidence angle of 13°, we give the corresponding spectra detected by placing the detector at different reflection angles η (Fig. 5). In the standard reflection setting, the two angles ϕ and γ are set to satisfy that $\phi + \gamma$ equals to 80°. The strongest intensities of peaks A1, A3, and B in cover scales occur in the detector covered reflection angular range (η of 18°–35°. Only a peak located at 400 nm was observed in the spectra of the ground scales, and the strongest reflectance occurs in the detector covered reflection angular range between 38° and 55°. It is far away from the standard 13° incidence setting. Therefore, it is un-
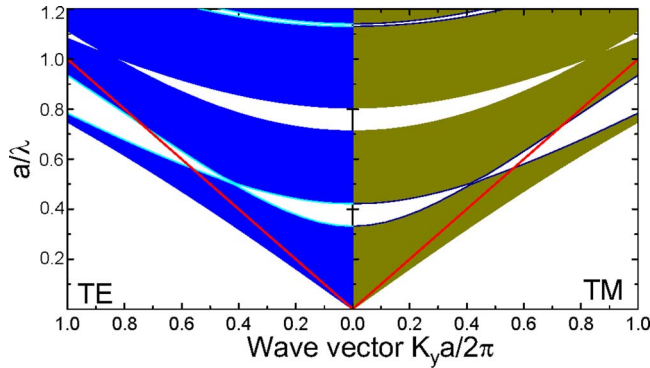
FIG. 6. (Color online) Calculated off-*x*-axis propagation band structure of the one-dimensional photonic structure (the shelf structure in scale ridges) using the MPB software.

derstandable why we cannot observe such a peak in its standard reflection spectra, such as in Fig. 4(c). Compared to peak B in Fig. 5(a), the peak in Fig. 5(b) is more symmetric and has an ~20 nm blueshift.

Peak B in the cover scale spectra and the sole peak in ground scale spectra can be interpreted using the shelve structures in their ridges, although the beams were reflected to different directions. Considering the shelve structure as a quasi-one-dimensional photonic structure, applying the MPB software package, we can calculate its photonic-band structure and the anticipated peaks in reflection spectra. Taking the parameter we measured from Fig. 3, the periodic distance (a) is 160 nm (90 nm plus 70 nm), while 90 and 70 nm are the thicknesses of the lamellar and air layers, respectively. We take the refractive index *n* of the wing materials as 1.56 following the experimental measurement.[16] By taking the normal direction of the shelves as *x*-axis, the band structures of both TE and TM modes related to off-*x*-axis propagation was calculated and displayed in Fig. 6. The red lines are the light lines. The shadowed region above the light lines gives the allowed modes propagating in air. The nonshadowed regions above light lines correspond to the band-gap related reflections. When the incidence beams are perpendicular to the shelf plane, the band-gap related reflection peak in visible light region will locate at around 425 nm. With the incidence beam direction deviates away from the perpendicular direction (corresponding to the increase in the *Y* component of the incidence wave vector in Fig. 6), the reflection peak will show a blueshift, which is consistent to our experimental results. The different situations in the cover and ground scales can be linked to the different inclination angles of the shelves with their scale planes. The different inclination angles make their actual incidence angles to be different. Keeping the 7° inclination angle of the cover scale in mind, ideally, relative to the normal direction of scale surface, the actual incident angle is 20° instead of 13°, then the strongest reflection from cover scales should appear around 27° (20° plus 7°), which falls in between the detection angles of 18°– 35°, as shown in Fig. 5(a). For the real incidence angle of ground scale in Fig. 5(b) is actual close to 30° (13° plus 17°), and then the band-gap related reflection should be reflected in the direction close to 47° (30° plus 17°) in reference to the scale surface, which is the right direction (38°–55°), where
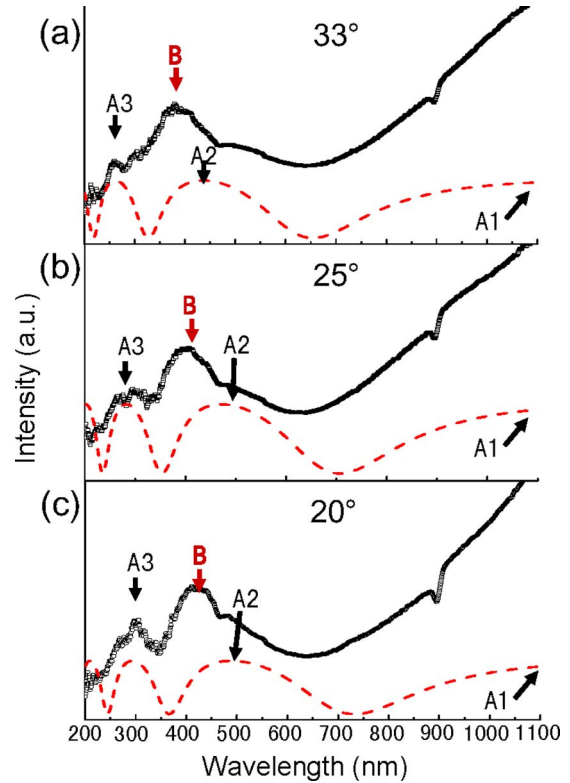

FIG. 7. (Color online) Incidence angle dependent reflection spectra of the cover scales. The incidence angles are 20°, 25°, and 33° from the tail direction in (a), (b), and (c), respectively, and the corresponding detector covered reflection angular ranges were 20°–35°, 23°–40°, and 30°–49°.

we observed the strongest reflection peak in Fig. 5(b). The blueshift of the peak from the ground scales compared to that from the cover scales is just related to its larger incidence angle.

More directly, we can calculate the orientation-dependent reflections through the one-dimensional PC by the Bragg reflection equation[24]

$$\lambda = 2d\sqrt{\varepsilon - \sin^2 \theta}, \tag{1}$$

where λ is the reflection peak related wavelength, *d* is the periodic parameter of the structure, θ is the incidence angle, the ε is the averaged dielectric constant, and it is

$$\varepsilon = n^2 \frac{90}{160} + 1\frac{70}{160} = 1.8064.$$

The reflection peak in Fig. 5(b) correspond to the incidence angle of 30° (13° plus 17°); therefore the calculated reflection peak is around 399 nm. For the real incident angle on cover scale in Fig. 5(a) is 20° and then the calculated reflection peak is around 416 nm. Both of them match well to what we have measured.

Figure 7 gives the orientation-dependent reflection spectra of the cover scales. The spectra in Figs. 7(a)–7(c) correspond to the incidence angles of 20°, 25°, and 33° from the tail direction, respectively. Table I gives the measured positions of each peak. Peak B has a good agreement with the prediction by the Bragg reflection equation. However, peaks A1 and A3 in the reflection spectra cannot be interpreted by the same token. Actually, they come from the thin film interference effect contributed by the base plate of the scales,

TABLE I. Experimental and calculated peaks in reflection spectra of cover scales. The inclination angle (7°) of the cover scale was considered in the calculation (* cannot be measured precisely from the spectra).

Peak	Incidence angle ∼20°		Incidence angle ∼25°		Incidence angle ∼33°	
	Measured	Calculated (nm)	Measured	Calculated (nm)	Measured	Calculated (nm)
A1	*	1466	*	1414	*	1351
A2	*	489	*	471	*	450
A3	288 nm	293	287 nm	283	259 nm	262
B	418 nm	405	397 nm	395	385 nm	377

such as the soap-bubble case.[3] The condition for the constructive interference between the beams reflected from the top and bottom surfaces of the base plate can be formulated as

$$2nd' \cos \theta = (m - 1/2)\lambda, \qquad (2)$$

where $d' = 250$ nm is the thickness of the base plate and m is an integer. The A1, A2, and A3 correspond to the reflection peaks with m equal to 1, 2, and 3, respectively. The calculated peaks corresponding to different incidence angles are also listed in Table I. At this point, the A3 peak has a good match with the ones measured in the experimental spectra. After considering the multiple reflections from the base plate, the amplitude of reflectivity can be given as[3]

$$r = r_{ab} - t_{ab}r_{ba}t_{ba}e^{i\phi}\kappa, \qquad (3)$$

where r_{ab} and t_{ab} are the reflectivity and transmittance amplitudes at the interface from the air to shelf. Here, $\kappa = 1/(1 - r_{ba}^2 e^{i\phi})$ and $\phi = 4\pi nd' \cos \theta / \lambda$. The simulated curves of the reflected intensity as given by $R = |r|^2$ for different incidence angles are plotted in Fig. 7 via red dashed lines. The asymmetric shoulder of peak B is due to the existence of peak A2 from the thin film interference effect of the base plate.

Different from the cover scales, the ground scales are covered heavily by the cross ribs and trabeculae. The incidence beam can hardly reach its base plate; even reached, the reflected beam has a high possibility to be scattered irregularly. Therefore, due to the screening effect of the cross ribs and trabeculae, the reflection peaks such as A1, A2, and A3 are missing in the reflection spectra of the ground scales.

IV. CONCLUSIONS

In this work, the reflection spectra from both cover and ground scales of *Morpho peleides* butterfly have been investigated. The structural origin of each reflection peak has been explored. Totally, four peaks—assigned as A1, A2, A3, and B—have been identified. The blue color related peak B is mainly contributed by the Bragg reflection from the shelf structure in the scale ridges. The A1, A2, and A3 peaks come from the thin film interference effect of the base plate. Due to the different inclination angles of the shelves relative to their scale planes, the beams with the same incidence angle will be reflected to different directions by the cover and ground scales. The missing of A1, A2, and A3 reflection peaks in the ground scales is due to the densely arranged cross ribs and

trabeculae on the scale, which screen the thin film interference effect contributed by its base plate.

Our study has provided a detailed interpretation regarding the nature of the reflections peaks in the reflection spectra from the butterfly wing. Such an understanding gives us an opportunity to deliberately modify the structure of a particular structural component using nanofabrication techniques so that unique optical properties can be tuned. This is a direction toward smart biophotonics that is composed of smart and functional materials, which are responsive to the environment such as electric field, humidity, and gases.

[1] J. D. Joannopoulos, S. G. Johnson, J. N. Winn, and R. D. Meade, *Photonic Crystals Molding the Flow of Light* (Princeton University Press, Princeton, NJ, 2008).
[2] C. Lopez, Adv. Mater. (Weinheim, Ger.) **15**, 1679 (2003).
[3] S. Kinoshita, S. Yoshioka, and J. Miyazaki, Rep. Prog. Phys. **71**, 076401 (2008).
[4] J. Y. Huang, X. D. Wang, and Z. L. Wang, Nano Lett. **6**, 2325 (2006).
[5] B. Gralak, G. Tayeb, and S. Enoch, Opt. Express **9**, 567 (2001).
[6] L. Plattner, J. R. Soc., Interface **1**, 49 (2004).
[7] S. Banerjee, J. B. Cole, and T. Yatagai, Micron **38**, 97 (2007).
[8] A. R. Parker, J. Opt. A, Pure Appl. Opt. **2**, R15 (2000).
[9] D. P. Gaillot, O. Deparis, V. Welch, B. K. Wagner, J. P. Vigneron, and C. J. Summers, Phys. Rev. E **78**, 031922 (2008).
[10] S. Yoshioka and S. Kinoshita, Proc. R. Soc. London, Ser. B **271**, 581 (2004).
[11] S. Yoshioka and S. Kinoshita, Proc. R. Soc. London, Ser. B **273**, 129 (2006).
[12] L. P. Biró, Zs. Bálint, K. Kertész, Z. Vértesy, G. I. Márk, Z. E. Horváth, J. Balázs, D. Méhn, I. Kiricsi, V. Lousse, and J.-P. Vigneron, Phys. Rev. E **67**, 021907 (2003).
[13] K. Watanabe, T. Hoshino, K. Kanda, Y. Haruyama, and S. Matsui, Jpn. J. Appl. Phys., Part 2 **44**, L48 (2005).
[14] K. Kertész, G. Molnár, Z. Vértesy, A. A. Koós, Z. E. Horváth, G. I. Márk, L. Tapasztó, Zs. Bálint, I. Tamáska, O. Deparis, J. P. Vigneron, and L. P. Biró, Mater. Sci. Eng., B **149**, 259 (2008).
[15] H. Ghiradella, Appl. Opt. **30**, 3492 (1991).
[16] P. Vukusic, J. R. Sambles, C. R. Lawrence, and R. J. Wootton, Proc. R. Soc. London, Ser. B **266**, 1403 (1999).
[17] S. Berthier, E. Charron, and J. Boulenguez, Insect Sci. **13**, 145 (2006).
[18] S. Yoshioka and S. Kinoshita, J. Opt. Soc. Am. A Opt. Image Sci. Vis **23**, 134 (2006).
[19] L. P. Biro, K. Kertesz, Z. Vertesy, G. I. Mark, Z. Balint, V. Lousse, and J. P. Vigneron, Mater. Sci. Eng., C **27**, 941 (2007).

[20] R. A. Potyrailo, H. Ghiradella, A. Vertiatchikh, K. Dovidenko, J. R. Cournoyer, and E. Olson, Nat. Photonics **1**, 123 (2007).

[21] W. Zhang, D. Zhang, T. X. Fan, J. J. Gu, R. Ding, H. Wang, Q. X. Guo, and H. Ogawa, Chem. Mater. **21**, 33 (2009).

[22] S. Kinoshita and S. Yoshioka, ChemPhysChem **6**, 1442 (2005).

[23] S. J. Johnson, J. D. Joannopoulos, and M. Soljačić, MIT Photonic Bands, see: http://ab-initio.mit.edu/wiki/index.php/MIT_Photonic_Bands, 2009.

[24] G. M. Gajiev, V. G. Golubev, D. A. Kurdyukov, A. V. Medvedev, A. B. Pevtsov, A. V. Sel'kin, and V. V. Travnikov, Phys. Rev. B **72**, 205115 (2005).